TÜBİTAK

**Turkish Journal of Biology**

**http://journals.tubitak.gov.tr/biology/**

**Research Article**

Turk J Biol
(2016) 40: 906-914

doi:10.3906/biy-1508-31

# Sodium borate treatment induces metabolic reprogramming in hepatocellular carcinoma through SIRT3 activation

**Berna ÜSTÜNER, Hüseyin ÇİMEN***
Department of Genetics & Bioengineering, Yeditepe Proteomics and Mass Spectrometry Laboratory (YediPROT), Yeditepe University, İstanbul, Turkey

**Received:** 10.08.2015 • **Accepted/Published Online:** 09.01.2016 • **Final Version:** 21.06.2016

**Abstract:** Sirtuins are $NAD^+$-dependent deacetylases and ADP ribosyltransferases that are activated under stress conditions such as calorie restriction and starvation. Boron, which is mostly found in the form of boric acid (BA) or sodium borate (NaB), is known to bind $NAD^+$. In this study, the effect of NaB on hepatoma cell line HEP3B was investigated by analyzing the proteins harvested from NaB-treated and serum-starved HEP3B cells. The NaB treatment (15 µg/mL) led to a decrease in the overall proteome acetylation and particularly in mitochondria, the synthesis rate of respiratory complexes, the amount of cellular reactive oxygen species, and the proliferation rate of HEP3B cells. On the other hand, the cellular ratio of $NAD^+$/NADH and the deacetylase activity of mitochondrial sirtuin, SIRT3, were found to be elevated. The results of this study suggest a link between boron treatment and activation of SIRT3 by means of a $NAD^+$–NaB interaction, which reprograms cellular metabolism. This study is expected to pave the way for new findings uncovering the metabolic changes in HEP3B cells related to SIRT3 activity upon NaB treatment.

**Key words**: Boron, sodium borate, sodium pentaborate pentahydrate, calorie restriction, NAD, mitochondria, acetylation, deacetylation, $NAD^+$-dependent deacetylase, Warburg effect

## 1. Introduction

Cancer cells mostly maintain higher rates of glycolysis by downregulating their oxidative phosphorylation (OXPHOS) regardless of environmental oxygen concentrations, a situation known as the Warburg effect. Decreased OXPHOS in cells displaying the Warburg effect is mostly associated with malfunctioning mitochondria (Chen and Russo, 2012), which is in turn related to cellular energy metabolism, maintained by the $NAD^+$/NADH ratio (Saunders and Verdin, 2007). The increased glucose uptake related to the Warburg effect not only serves as a source of ATP generation through the tricarboxylic acid (TCA) cycle, but also as a source of carbon and metabolites harnessed in the synthesis of macromolecules supporting cellular proliferation (Huang et al., 2014). This is predominantly seen in fast-growing tumor cells (Jose et al., 2011) such as hepatoma, providing a growth advantage over healthy cells as they become less exposed to oxidative stress by avoiding high levels of reactive oxygen species (ROS) (Kondoh et al., 2007; Sosa et al., 2013). Hepatocellular carcinoma (HCC) is a type of liver cancer, which primarily results from viral hepatitis B infection. Pathways related to immunity, cell cycle, protein metabolism, translation, glycolysis, and OXPHOS are especially altered in HBV-induced HCC (Lee et al., 2012). Additionally, enhanced generation and accumulation of ROS is lethal for cells through cellular mechanisms. This includes oxidative damage to cellular components, which in turn affects cellular proliferation, apoptosis, tissue invasion, and metastasis (Sosa et al., 2013). Compared to normal cells, tumorigenic cells can endure high levels of ROS by inducing new redox balances within their metabolisms. In this way, cancer cells have the capacity to survive against free radical damage through reprogramming their metabolic rate and increasing proliferation (Sosa et al., 2013). Mitochondria have a great impact on tumor cell survival by mediating apoptotic pathways (Gogvadze et al., 2008); the maintenance of mitochondrial potential and oxidative equilibrium controls the cell viability. Loss of structural integrity in the mitochondrial inner membrane and disruption of OXPHOS machinery leads to an impairment of membrane potential (Verdin et al., 2010). Mitochondrial function is tightly controlled by posttranslational modifications (PTMs) such as acetylation and phosphorylation (Koc and Koc, 2012; Newman et al., 2012; Padrao et al., 2013). The most common and crucial type of PTM taking place

* Correspondence: huseyin.cimen@yeditepe.edu.tr

in mitochondria is lysine acetylation, which occurs in proteins involved in metabolic regulations (Kim et al., 2006; Choudhary et al., 2009; Close et al., 2010; Wang et al., 2010; Zhao et al., 2010; Hirschey et al., 2011). Sirtuins are redox-sensitive and one of the main regulators of lifespan in response to stress (Hubbard and Sinclair, 2014). They regulate the acetylation state of histones, transcription factors, and additional nonhistone protein targets implicated in the expression of genes involved in stress response, energy metabolism, and longevity (Suchankova et al., 2009). Having the most robust mitochondrial deacetylase activity, SIRT3 is the primary regulator of lysine acetylation in mitochondria (Amado et al., 2014). Nutrient starvation induces elevated levels of $NAD^+$ leading to increased activity of SIRT3 and a shift away from liver glycolysis upon calorie restriction (Brosnan, 2000). Boron, which is one of the highly beneficial trace elements for humans, animals, and plants, is widely distributed in nature and is released by natural processes (Hunt and Idso, 1999). It is an active inducer of the immune system and is known to bind to $NAD^+$ through reactions involving the hydroxyl groups on pyridine nucleotides (Hunt and Idso, 1999). In this study, we have investigated how the interaction of sodium borate (NaB) with $NAD^+$ might alter the intracellular $NAD^+$/NADH ratio and affect the cellular level of ROS and SIRT3 activity in HEP3B, an HCC cell line.

## 2. Materials and methods

### 2.1. Cell culture and boron treatment

HEP3B, human hepatoma cells, were cultured in Dulbecco's modified Eagle's medium (DMEM) (GIBCO, Germany) in the presence of 10% (v/v) fetal bovine serum (GIBCO) and 1% penicillin–streptomycin (GIBCO) at 37 °C and 5% $CO_2$. The HEP3B cells were treated with NaB (sodium pentaborate pentahydrate from Boren, Turkey) in low-glucose (1 g/L) DMEM (GIBCO) for 72 h and starved for serum for the last 24 h.

### 2.2. Protein amount measurement

Protein extraction from cells was prepared with the RIPA lysis buffer system (Santa Cruz Biotechnology, USA) supplemented with 2 mM PMSF, 1X protease inhibitor cocktail, and 1 mM sodium orthovanadate (Santa Cruz Biotechnology). Protein amounts of cell lysates were determined using the Pierce BCA Protein Assay Kit (Pierce Biotechnology, USA), using bovine serum albumin as a standard.

### 2.3. Isolation of mitochondrial fraction

Mitochondria were isolated from HEP3B cells ($8 \times 10^7$) treated with 15 μg/mL NaB for 72 h by employing a protocol modified from Cimen et al. (2010). Cell pellets were resuspended in isolation buffer containing 26 mM sucrose (Carlo Erba, Italy), 50 mM Tris-HCl (pH 7.6; MP-Biomedicals, USA), 40 mM KCl (Merck, Germany), 20 mM $MgCl_2$ (Merck), 0.8 mM EDTA (Merck), and 6 mM β-mercaptoethanol (Merck), supplemented with 0.1% (w/v) PMSF (Roche, Switzerland). After separating the cytosolic fraction, the remaining pellets were resuspended in wash buffer (50 mM Tris-HCl, pH 7.6; 40 mM KCl; 20 mM $MgCl_2$; 1 mM DTT) supplemented with 0.1% (w/v) PMSF. Pellets were obtained by centrifuging twice, at 12,000 × *g* and 4 °C for 10 min. Percent relative acetylation of mitochondrial protein samples was calculated by normalizing the obtained quantitative acetylation data. Each quantitation was initially done using the control sample (0 μg/mL) as a reference. The amount of acetylation signal of each sample was then divided by the amount of respective control signals. GAPDH mouse monoclonal antibody (1:5000) and HSP60 mouse monoclonal antibody (1:5000) were blotted onto the same PVDF membrane as control antibodies.

### 2.4. Immunoblotting

Protein samples harvested from HEP3B cells were loaded onto SDS-polyacrylamide gel and transferred to a polyvinylidene difluoride membrane (PVDF). Protein in the amount of 20 μg was loaded for each sample to be analyzed. For acetylome profiling, the blot was probed with an acetylated lysine monoclonal antibody (Cell Signaling, USA) at 1:1000 dilution, glyceraldehyde 3-phosphate dehydrogenase (GAPDH) mouse monoclonal antibody (Abcam, UK) at 1:5000 dilution, and heat-shock protein 60 (HSP60) mouse monoclonal antibody (Cell Signaling) at 1:5000 dilution. Percent relative acetylation of whole-cell lysate protein samples was calculated by normalizing the obtained quantitative acetylation data. Each quantitation was done initially using the control sample (0 μg/mL) as a reference. The amount of acetylation signal of each sample was then divided by the amount of respective control signals. To analyze the OXPHOS enzyme complexes, the blot was probed with Total OXPHOS Rodent WB Antibody Cocktail (Abcam) and HSP60 mouse monoclonal antibody (Cell Signaling) at 1:5000 dilutions. Secondary antibody for acetylation was antirabbit IgG (Sigma-Aldrich, USA) at 1:2500 dilution and antimouse IgG (Sigma-Aldrich) at 1:5000 dilution for GAPDH, HSP60, and OXPHOS profiling. Imaging was performed using the BIO-RAD ChemiDoc XRS + Molecular Imager with Lab Software.

### 2.5. Intracellular $NAD^+$/NADH ratio measurement

The intracellular $NAD^+$/NADH ratio of NaB-treated HEP3B cells was determined using the $NAD^+$/NADH Assay Kit (Abcam). The kit contains a specific enzyme mix that creates a cyclic reaction in which the oxidized form of nicotinamide dinucleotide, $NAD^+$, and its reduced form, NADH, are constantly being produced and metabolized. The kit is designed to specifically detect NADH and NAD, so the intracellular ratio of $NAD^+$ to NADH can

be calculated accordingly. HEP3B cells were cultured and treated in 6-well plates. Cells ($1.5 \times 10^6$) were harvested for each sample and the assay was performed immediately after a cold PBS rinse followed by application of $NAD^+$/NADH extraction buffer. Cellular $NAD^+$/NADH ratio was determined by separately measuring the NAD total (NADt) and NADH amounts in cultured HEP3B cells harvested after treatment with 15 μg/mL NaB for 72 h in combination with starvation applied for the last 24 h. $NAD^+$/NADH ratios were then calculated using NADH and NADt amounts. The amount of NADH was detected at 450 nm using the BIO-TEK EL × 800 Microplate Reader.

**2.6. Cell viability assay**

The viability of treated cells was investigated using the CellTiter96 Aqueous Non-Radioactive Cell Proliferation Assay (Promega, USA). Cells (1000 per well) were inoculated into a 96-well plate in high-glucose DMEM media containing 10% FBS and 1% penicillin–streptomycin. NaB treatment (15 μg/mL) in low-glucose DMEM media containing 10% FBS and 1% penicillin–streptomycin was initiated on day 2, prior to measurement. Starvation in combination with 15 μg/mL NaB treatment in serum-free low-glucose DMEM media was performed after the measurement on day 3. For the absorbance measurements, the BIO-TEK EL × 800 Microplate Reader was used. Results were calculated by taking the average of absorbance values of each sample in triplicate. Data were normalized based on absorbance results obtained on the initial day of the experiment.

**2.7. Cellular ROS detection**

Cellular ROS detection was performed in the presence of a cell permeant reagent, 2',7'-dichlorofluorescein diacetate (DCFDA), using the DCFDA Cellular ROS Detection Assay Kit (Abcam). HEP3B cells ($5 \times 10^4$) treated in a 6-well plate were harvested for each sample to be analyzed with the BD FACSCalibur Flow Cytometer at excitation of 495 nm and emission of 529 nm. Percent decrease in ROS level in HEP3B cells treated with 15 μg/mL NaB was compared to nontreated cells.

**2.8. SIRT3 activity assay**

The effect of NaB (15 μg/mL) on SIRT3 activity was determined using the SIRT3 Deacetylase Fluorometric Assay Kit (CycLex, Japan). Measurements were done using the BC BIOTEK FL × 800 TBID fluorometric microplate reader at excitation of 460 nm and emission of 360 nm. The reaction was performed by measuring SIRT3 deacetylase activity on a fluoro-substrate peptide added to the mixture. Specific activity of SIRT3 was calculated using fluorescence intensity values obtained in the initial 20 min of reaction, according to the data obtained from a fluorometric microplate reader.

**2.9. Statistical analysis**

The statistical significance of each experimental result was analyzed by running an unpaired t-test from the averaged data obtained from 3 independent experiments using GraphPad Software. $P < 0.05$ from 3 independent experiments was taken as significant.

## 3. Results

**3.1. NaB treatment decreases proteome acetylation**

HEP3B cells were initially treated with NaB concentrations of 0, 10, 15, and 20 μg/mL for 72 h in combination with serum starvation in the last 24 h in order to determine the effective treatment concentration for further experiments (Figure 1A). According to the statistical analysis obtained from 3 independent experiments with immunoblotting study of total protein extracts with an antibody against the ε-amino group of the lysine residue, significant decreases of 29% and 19% were detected in the protein samples prepared from cells treated with 15 μg/mL NaB compared to other concentrations (Figures 1A and 1B).

**3.2. Cellular $NAD^+$/NADH ratio increases upon NaB treatment**

The cellular $NAD^+$/NADH ratio was determined by separately measuring NADt and NADH amounts in cultured HEP3B cells harvested after treatment with 15 μg/mL NaB for 72 h in combination with starvation. In order to measure the NADH amounts, samples were heated at 60 °C to decompose NAD. $NAD^+$/NADH ratios were then calculated by subtracting NADH from NADt and dividing the outcome by NADH. According to the results obtained at 450 nm, 15 μg/mL NaB treatment decreased the $NAD^+$ level by 14% and the NADH level by 53%. The cellular $NAD^+$/NADH ratio, however, doubled in cultured HEP3B cells ($P < 0.05$) (Figure 2).

**3.3. Mitochondrial proteins are deacetylated upon NaB treatment**

Mitochondria were isolated from HEP3B cells treated with 15 μg/mL NaB and lysed for protein study. Immunoblotting analysis of the samples separated by 10% SDS-PAGE revealed a statistically significant decrease of 11% in mitochondrial proteome acetylation ($P < 0.05$) (Figure 3A). The results obtained from the mitochondrial HSP60 antibody signal and cytoplasmic GAPDH antibody signal showed that the mitochondria of the 15 μg/mL NaB-treated samples and control samples were successfully isolated (Figure 3B).

**3.4. Protein synthesis decreases in OXPHOS machinery upon NaB treatment**

To analyze proteins related to oxidative phosphorylation machinery, the amount of enzyme complexes involved in this energy generation pathway was investigated upon NaB treatment. According to the immunoblotting results

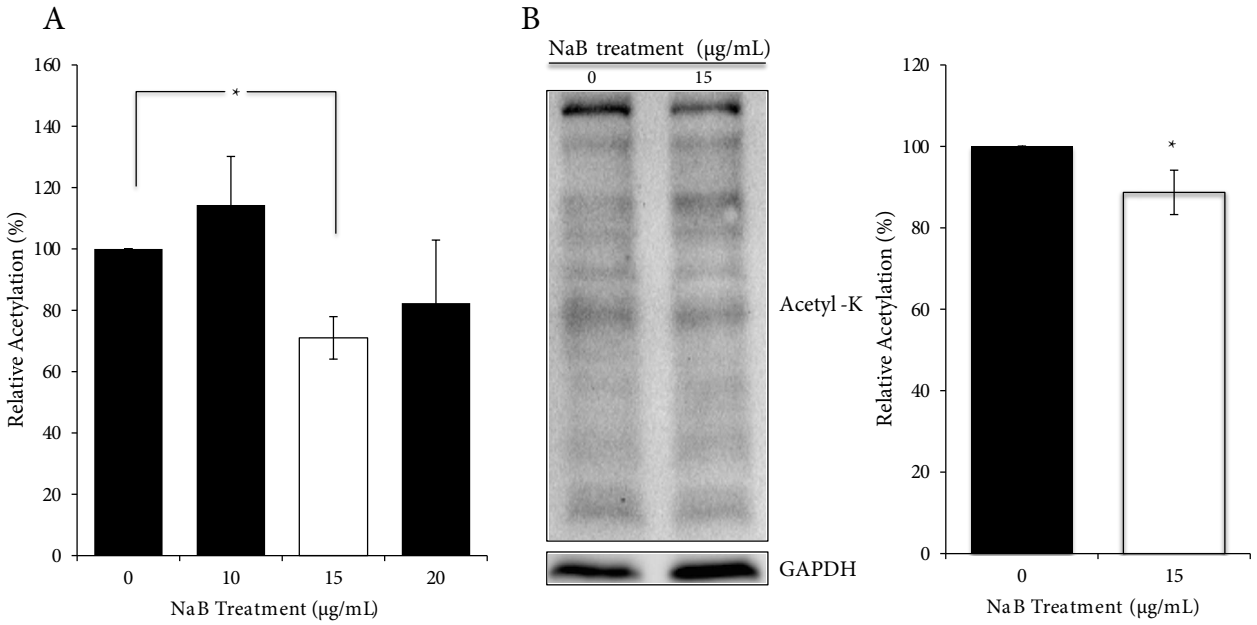


**Figure 1.** NaB treatment decreases proteome acetylation. (A) Relative ratio of acetylation level to control (β-actin) in whole-cell lysate proteins from HEP3B cells treated with NaB. (B) Acetylation and GAPDH signals of control and 15 μg/mL NaB treated whole cell lysate proteins. *: $P < 0.05$.

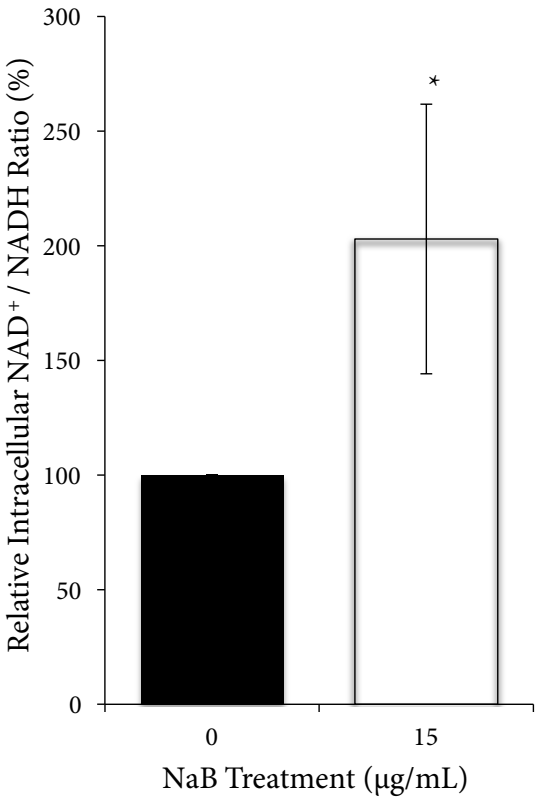


**Figure 2.** Cellular $NAD^+$/NADH ratio is increased upon NaB treatment. Intracellular $NAD^+$/NADH ratios of cultured HEP3B cells treated with NaB. *: $P < 0.05$.

following SDS-PAGE separation, a significant reduction was observed in the OXPHOS complex subunits: 17%, 24%, 22%, 11%, and 13% in CI (complex I, NADH dehydrogenase subunit NDUFB8), CII (complex II, succinate dehydrogenase subunit SDHB), CIII (complex III, cytochrome *c* oxidoreductase subunit UQCRC2), CIV (complex IV, cytochrome *c* oxidase subunit MTCO1), and CV (complex V, ATP synthase subunit ATPSA), respectively ($P < 0.05$) (Figure 4A). Further analysis of CIV confirmed that the synthesis of this mitochondrial encoded complex subunit (MTCO1) decreased by 11% when HSP60 antibody was used as the loading control (Figure 4B).

### 3.5. NaB treatment reduced HEP3B cancer cell proliferation

Cellular proliferation of HEP3B cells was determined in the presence of the inner salt (MTS, 3-(4,5-dimethylthiazol-2-yl)-5-(3-carboxymethoxyphenyl)-2-(4-sulfophenyl)-2H-tetrazolium) and the intermediate electron acceptor (PMS, phenazine methosulfate). One thousand cells per well were inoculated into a 96-well plate. The NaB treatment was initiated after the day 1 measurement of cell viability. Serum starvation in combination with the 15 μg/mL NaB treatment was applied after the day 3 measurement of cell viability. The results obtained over 4 days demonstrated that cancer cell proliferation was reduced by 33%, 20%, and 32% on days 2, 3, and 4, respectively, upon 15 μg/mL NaB treatment ($P < 0.05$) (Figure 5A).

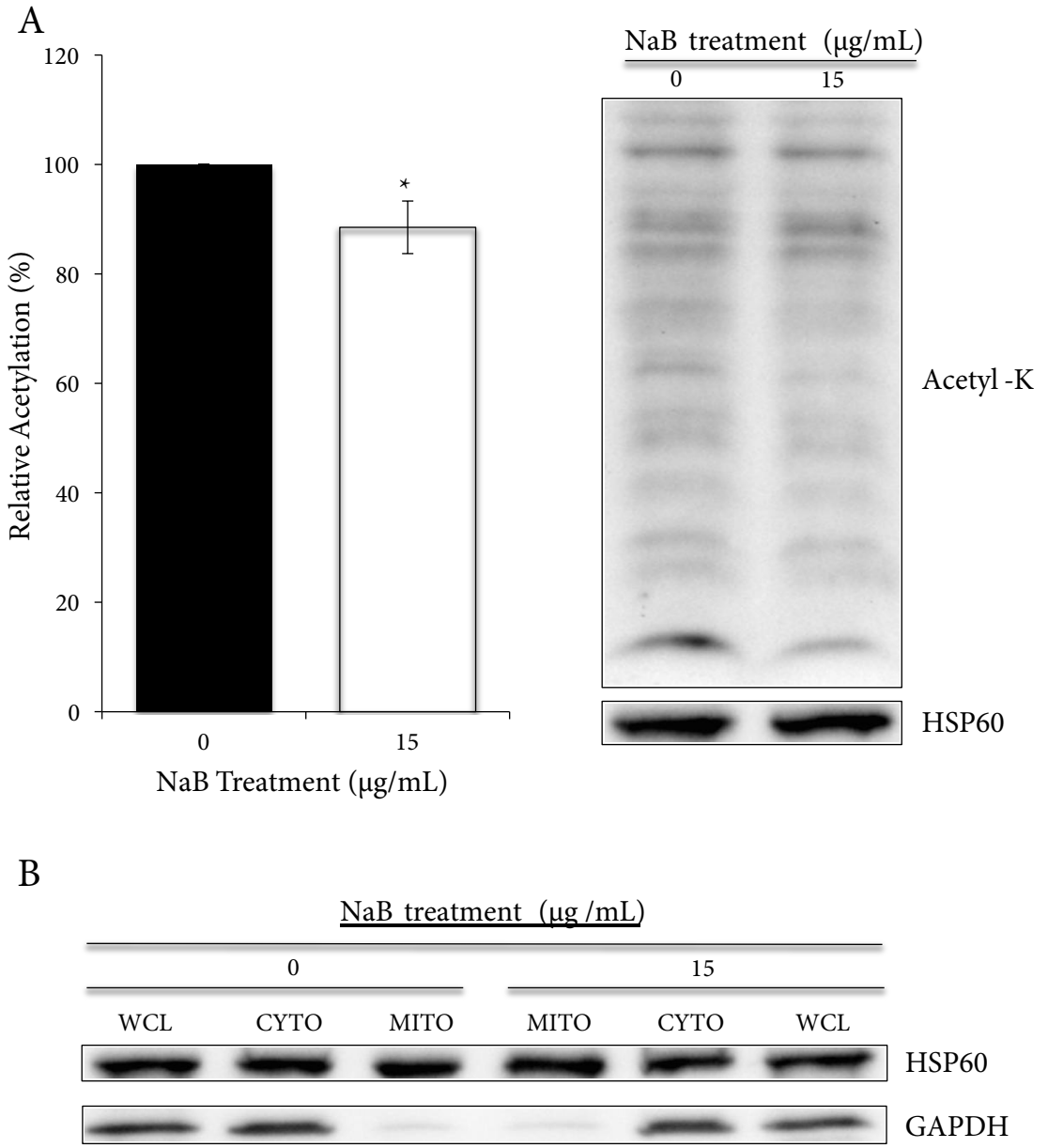


**Figure 3.** Mitochondrial proteins are deacetylated upon NaB treatment. (A) Relative ratio of acetylation level to control (HSP60) in mitochondrial proteins from HEP3B cells treated with NaB. (B) GAPDH and HSP60 signals of control and 15 µg/mL NaB-treated whole-cell lysate (WCL), cytosolic fraction (CYTO), and mitochondrial (MITO) proteins.

**3.6. Cellular ROS levels are reduced upon NaB treatment**

Cellular ROS activity was measured depending on the activity of cellular esterases that deacetylate DCFDA to a nonfluorescent compound, which is then oxidized to a highly fluorescent compound, 2',7'-dichlorofluorescein (DCF), by ROS. The fluorescence intensity of samples was measured at an excitation of 485 nm and an emission of 535 nm. According to the fluorescence data obtained by a flow cytometer from 3 independent experiments, 15 µg/mL NaB treatment for 72 h in combination with 24 h of starvation decreased cellular ROS levels by 73% in HEP3B cells ($P < 0.05$) (Figure 5B).

**3.7. NaB treatment enhanced SIRT3 deacetylase activity**

SIRT3 enzymatic activity was determined by measuring its deacetylase activity on a fluoro-substrate peptide added to the reaction mixture. The fluorescence intensities of samples were measured at an excitation of 360 nm and an emission of 460 nm. Specific activity of SIRT3 was

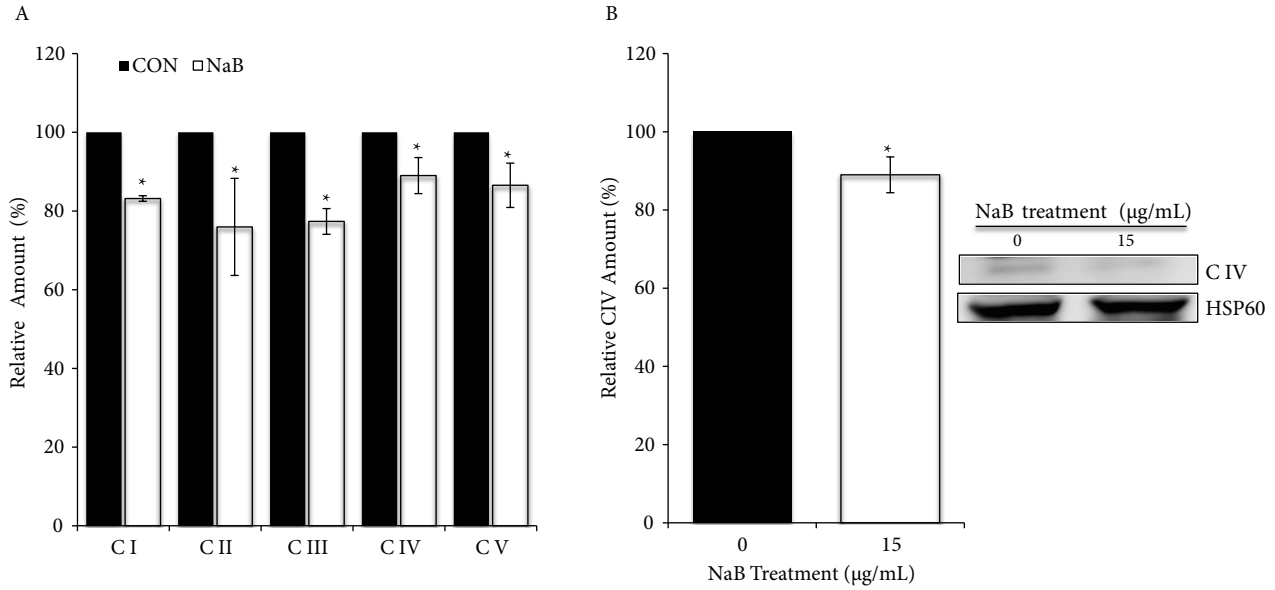


**Figure 4.** (A) Protein synthesis is decreased in OXPHOS machinery upon NaB treatment. Relative ratios of OXPHOS complex enzyme levels to control (HSP60) in mitochondrial proteins from HEP3B cells treated with NaB. (B) Relative ratio of complex IV level to control (HSP60) in mitochondrial proteins from HEP3B cells treated with 15 μg/mL NaB. *: $P < 0.05$.

calculated using the fluorescence intensity values obtained during the initial 20 min of reaction. Data showed that NaB significantly enhanced SIRT3 deacetylase activity by 31% in HEP3B cells treated with 15 μg/mL NaB, compared to cells without treatment ($P < 0.05$) (Figure 5C).

## 4. Discussion

Most cancer cells are devoid of functional mitochondria. They exhibit high ROS generation, reduced mitochondrial enzyme activity, decreased levels of OXPHOS-derived ATP, and increased acetylation of proteins regulating metabolic gene regulation. These functional impairments in mitochondria result in the Warburg effect, which is demonstrated with enhanced glycolytic rate.

In this study, the impact of NaB-$NAD^+$ interaction on the activity of the stress-responsive mitochondrial deacetylase SIRT3 was investigated. NaB was used to alter the intracellular levels of $NAD^+$ via chemical interaction. This interaction, together with nutritional stress, modulated SIRT3 deacetylase activity (Merksamer et al., 2013). Given the importance of protein functioning in coordinating metabolic pathways, the cellular energy hubs, mitochondria, were targeted by this combined treatment strategy. The aim was to reprogram the metabolism of HEP3B human HCC cells by means of NaB treatment in order to reverse the Warburg effect by restoring proper mitochondrial function.

Immunoblotting analyses were performed to investigate the acetylome of the proteins harvested from HEP3B cells. Following an initial broad range analysis with 0–25 μg/mL NaB concentrations (Figure 1A), the applied concentration was narrowed down to 15 μg/mL NaB (Figure 1B). Immunoblotting analyses on 6 independent sample groups revealed a significant decrease of 29% in proteome acetylation of samples treated with 15 μg/mL NaB (Figure 1A). Since the NaB treatment of 15 μg/mL was considered to be an ideal concentration for the changes in the acetylome of samples, experiments were further carried out using this NaB concentration as the effective dose (Figure 1B). Next, in order to confirm the interaction between NaB and $NAD^+$, the relative intracellular NAD+/NADH ratio was investigated. Three independent analyses showed that the intracellular $NAD^+$/NADH ratio in HEP3B cells increased by 100% upon treatment of cells with 15 μg/mL NaB combined with 24 h of starvation (Figure 2). This result confirmed that the decrease in overall protein acetylation observed in whole-cell lysate proteins was in fact related to NaB-$NAD^+$ interaction and brought up the possibility of an improved cellular redox state achieved through the functioning of metabolic proteins. Analyses were directed towards the proteome of the cellular center of energetic pathways, the mitochondria.

In order to analyze the mitochondrial proteome, fractionation of mitochondria was initially performed by employing a Dounce homogenizer. Immunoblotting analysis of the mitochondrial proteome revealed a significant decrease of 11% in the overall mitochondrial protein acetylation (Figure 3A). Specific antibodies of the mitochondrial protein HSP60 and the cytosolic protein GAPDH served as controls of the isolation process (Figure

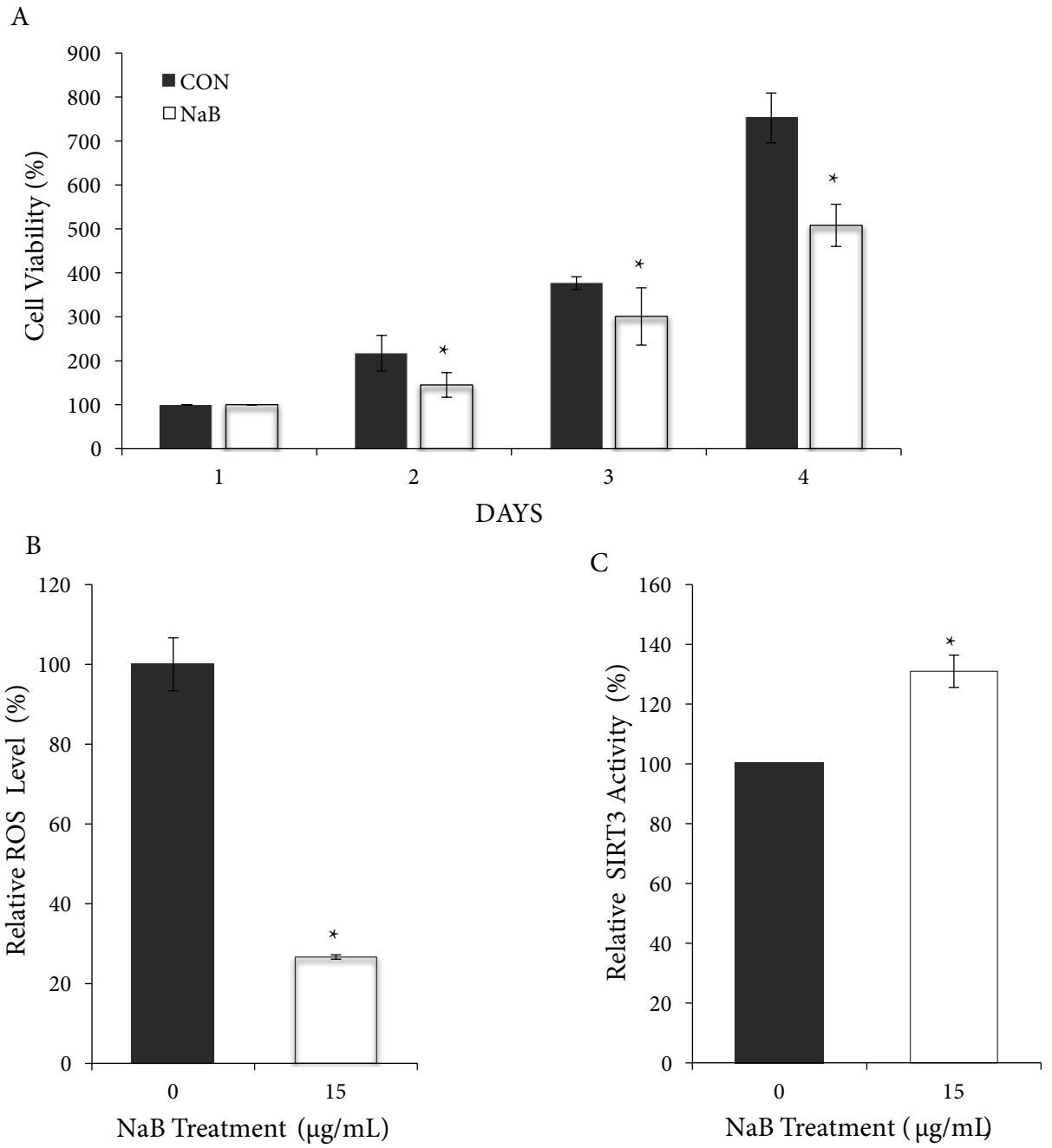


**Figure 5.** (A) NaB treatment reduced HEP3B cancer cell proliferation. Percent cell viability measured through metabolic activity of cultured HEP3B cells treated with 15 µg/mL NaB. (B) Cellular ROS levels are reduced upon NaB treatment. (C) Relative SIRT3 activity is increased upon NaB treatment. *: $P < 0.05$.

3B). Thus, the NaB treatment was shown to be effective in reducing the mitochondrial proteome acetylation, as expected. This posttranslational alteration might have an impact on the synthesis of mitochondrial proteins that would further provide an insight into mitochondrial biogenesis. Given their pivotal roles in energy generation, the analyses of mitochondrial protein synthesis were preferentially carried out on the proteins involved in the mitochondrial OXPHOS pathway. NDUFB8 (CI), SDHB (CII), UQCRC2 (CIII), MTCOI (CIV), and ATPSA (CV), the subunits of the OXPHOS complexes, were examined by immunoblotting assay using the MitoProfile Total OXPHOS Rodent Antibody Cocktail. According to the analysis, a 17%, 24%, 22%, 11%, and 13% decrease was

observed in the amounts of CI, CII, CIII, CIV, and CV proteins, respectively (Figure 4A). The relative changes in these subunits were calculated using HSP60 as a loading control on the gels (Figure 4B). In addition, MTCOI is one of the mitochondrial encoded subunits of mitochondrial cytochrome *c* oxidase (CIV) and is synthesized by mitochondrial ribosomes (Yang et al., 2010). The decrease in the amount of MTCOI is in agreement with the finding that mitochondrial ribosomes are acetylated and the reduced acetylation level of ribosomal proteins results in a lower rate of protein synthesis in the mitochondria (Yang et al., 2010).

An overall reduction in the synthesis of proteins responsible for ATP generation also indicates a reduction in mitochondrial biogenesis. A decline in cellular proliferation rate would be expected in light of this result, which was investigated via cell viability assay. According to the results obtained, a significant reduction of 33%, 20%, and 32% in cellular proliferation rates was observed on days 2, 3, and 4 after treatment with 15 µg/mL NaB, respectively (Figure 5A). Together with the results of OXPHOS subunit synthesis, a decline in mitochondrial biogenesis was confirmed.

This finding could indicate a functional restoration of mitochondrial content in hepatoma cancer cells upon NaB treatment by means of increasing the mitochondrial quality via recycling of troubled mitochondria. For further analyses, the level of ROS, a major factor contributing to mitochondrial damage, was investigated in HEP3B cells. Cellular ROS detection revealed a significant decrease (73%) in the level of ROS in HEP3B cells treated with 15 µg/mL NaB (Figure 5B). This result verified that mitochondrial functioning was indeed restored upon NaB treatment, and mitochondrial content of HEP3B cells was more resistant to free radical damage.

Lastly, in order to certify that the mitochondrial deacetylase enzyme SIRT3 was in fact responsible for this functional restoration and metabolic reprogramming, the specific activity of SIRT3 was determined in the presence of a protease (lysyl endopeptidase) that releases fluorophore-attached fragments from a substrate peptide. The intensity of fluorescent signals coming from these fragments was the measure of SIRT3 activity. The results showed that SIRT3 deacetylase activity was significantly enhanced by 31% upon treatment with 15 µg/mL NaB (Figure 5C).

All together, these results indicate that NaB treatment in combination with calorie restriction is effective in inducing SIRT3 activation through $NAD^+$ interaction. This combined treatment strategy involving NaB treatment and calorie restriction is shown to be successful in achieving metabolic regulation through modifying mitochondrial protein acetylation in human hepatocellular carcinoma. For this reason, it is applicable to improve NaB-based products to enhance the efficiency of treatments against hepatocellular carcinoma.

**Acknowledgments**

This study was supported by Yeditepe University. We thank Prof Dr Fikrettin Şahin, the head of the Genetics and Bioengineering Department at Yeditepe University, for supplying sodium borate (sodium pentaborate pentahydrate) and the available facilities.

## References

Amado FM, Barros A, Azevedo AL, Vitorino R, Ferreira R (2014). An integrated perspective and functional impact of the mitochondrial acetylome. Expert Rev Proteomic 11: 383-394.

Brosnan JT (2000). Glutamate, at the interface between amino acid and carbohydrate metabolism. J Nutr 130: 988S-990S.

Chen JQ, Russo J (2012). Dysregulation of glucose transport, glycolysis, TCA cycle, and glutaminolysis by oncogenes and tumor suppressors in cancer cells. Biochim Biophys Acta 1826: 370-384.

Choudhary C, Kumar C, Gnad F, Nielsen ML, Rehman M, Walther TC, Olsen JV, Mann M (2009). Lysine acetylation targets protein complexes and co-regulates major cellular functions. Science 325: 834-840.

Cimen H, Han MJ, Yang Y, Tong Q, Koc H, Koc EC (2010). Regulation of succinate dehydrogenase activity by SIRT3 in mammalian mitochondria. Biochemistry 49: 304-311.

Close P, Creppe C, Gillard M, Ladang A, Chapelle JP, Nguyen L, Chariot A (2010). The emerging role of lysine acetylation of non-nuclear proteins. Cell Mol Life Sci 67: 1255-1264.

Gogvadze V, Orrenius S, Zhivotovsky B (2008). Mitochondria in cancer cells: what is so special about them? Trends Cell Biol 18: 165-173.

Hirschey MD, Shimazu T, Jing E, Grueter CA, Collins AM, Aouizerat B, Stancakova A, Goetzman E, Lam MM, Schwer B et al. (2011). SIRT3 deficiency and mitochondrial protein hyperacetylation accelerate the development of the metabolic syndrome. Mol Cell 44: 177-190.

Huang W, Wang Z, Lei QY (2014). Acetylation control of metabolic enzymes in cancer: an updated version. Acta Bioch Bioph Sin 46: 204-213.

Hubbard BP, Sinclair DA (2014). Small molecule SIRT1 activators for the treatment of aging and age-related diseases. Trends Pharmacol Sci 35: 146-154.

Hunt CD, Idso JP (1999). Dietary boron as a physiological regulator of the normal inflammatory response: a review and current research progress. J Trace Elem Exp Med 12: 221-233.

Jose C, Bellance N, Rossignol R (2011). Choosing between glycolysis and oxidative phosphorylation: a tumor's dilemma? Biochim Biophys Acta 1807: 552-561.

Kim SC, Sprung R, Chen Y, Xu Y, Ball H, Pei J, Cheng T, Kho Y, Xiao H, Xiao L et al. (2006). Substrate and functional diversity of lysine acetylation revealed by a proteomics survey. Mol Cell 23: 607-618.

Koc EC, Koc H (2012). Regulation of mammalian mitochondrial translation by post-translational modifications. Biochim Biophys Acta 1819: 1055-1066.

Kondoh H, Lleonart ME, Bernard D, Gil J (2007). Protection from oxidative stress by enhanced glycolysis; a possible mechanism of cellular immortalization. Histol Histopathol 22: 85-90.

Lee SY, Song MH, Koo I, Lee KH, Suh KS, Kim BY (2012). Comparison of pathways associated with hepatitis B- and C-infected hepatocellular carcinoma using pathway-based class discrimination method. Genomics 99: 347-354.

Merksamer PI, Liu Y, He W, Hirschey MD, Chen D, Verdin E (2013). The sirtuins, oxidative stress and aging: an emerging link. Aging 5: 144-150.

Newman JC, He W, Verdin E (2012). Mitochondrial protein acylation and intermediary metabolism: regulation by sirtuins and implications for metabolic disease. J Biol Chem 287: 42436-42443.

Padrao AI, Vitorino R, Duarte JA, Ferreira R, Amado F (2013). Unraveling the phosphoproteome dynamics in mammal mitochondria from a network perspective. J Proteome Res 12: 4257-4267.

Saunders L, Verdin E (2007). Sirtuins: critical regulators at the crossroads between cancer and aging. Oncogene 26: 5489-5504.

Sosa V, Moline T, Somoza R, Paciucci R, Kondoh H, Lleonart ME (2013). Oxidative stress and cancer: an overview. Ageing Res Rev 12: 376-390.

Suchankova G, Nelson LE, Gerhart-Hines Z, Kelly M, Gauthier MS, Saha AK, Ido Y, Puigserver P, Ruderman NB (2009). Concurrent regulation of AMP-activated protein kinase and SIRT1 in mammalian cells. Biochem Bioph Res Co 378: 836-841.

Verdin E, Hirschey MD, Finley LW, Haigis MC (2010). Sirtuin regulation of mitochondria: energy production, apoptosis, and signaling. Trends Biochem Sci 35: 669-675.

Wang Q, Zhang Y, Yang C, Xiong H, Lin Y, Yao J, Li H, Xie L, Zhao W, Yao Y et al. (2010). Acetylation of metabolic enzymes coordinates carbon source utilization and metabolic flux. Science 327: 1004-1007.

Yang Y, Cimen H, Han MJ, Shi T, Deng JH, Koc H, Palacios OM, Montier L, Bai Y, Tong Q et al. (2010). NAD+-dependent deacetylase SIRT3 regulates mitochondrial protein synthesis by deacetylation of the ribosomal protein MRPL10. J Biol Chem 285: 7417-7429.

Zhao S, Xu W, Jiang W, Yu W, Lin Y, Zhang T, Yao J, Zhou L, Zeng Y, Li H et al. (2010). Regulation of cellular metabolism by protein lysine acetylation. Science 327: 1000-1004.